Millimeter Wave Propagation in Arid Land—A Field Study in Riyadh

Adel A. Ali and Mohammed A. Alhaider, *Senior Member, IEEE*

Abstract—**A field study on wave propagation covering a wide range of the electromagnetic spectrum was actively running for four years in the city of Riyadh, Saudi Arabia. The region can be considered as a typical arid climate where the rate of evaporation is higher than the rate of precipitation. The study involves the operation and continuous, computerized monitoring of two millimetric wave links with radio frequency of 40 GHz, and an infrared link with 0.88 μm wavelength. A meteorological station is also operated and monitored. This paper presents a description of the experiment, and reports results of measuring sand storms and rain as they affect the radiowave propagation at 40 GHz and at near infrared. The effect of sand storms on propagation is studied by measuring the storm parameters; viz., visibility, particle size and size distribution, and induced attenuation due to these storms. The results are compared with long-term visibility data for Riyadh, and complete statistical analysis are given. The effect of rain is studied by measuring both rain rate and rain attenuation. Long-term rain data are utilized to derive long-term rain statistics. It is shown in particular that the measured attenuation caused by sand storms is about four times larger than the calculated attenuation at 40 GHz. The measured rain attenuation at infrared is found to be smaller by a factor of 0.3 than theoretically predicted attenuation.**

I. Introduction

THE present trend in radio design calls for the use of frequencies above 30 GHz for short links carrying wide-band digital communication signals. A hop length of 3–5 km may be considered for climatic regions dominated by heavy rain. Site (route) diversity and frequency diversity [1], [2] are expected to provide protection against attenuation by rainfall. A major problem with the short hop system is attributed to the noise accumulated in the tandem repeaters. However, digital modulation with regeneration at each repeater will solve the problem. Here the limiting design factor may not be rainfall attenuation, rather, equipment reliability will set the limit on system performance.

In Saudi Arabia and similar areas with little rainfall, much longer hops may be feasible. Besides rainfall, propagation of millimetric waves is marked by many other phenomena such as bandwidth decoherence [3] and depolarization or polarization rotation. Since all the above phenomena are weather dependent, their effect on propagation should be evaluated for the particular transmission climate.

Manuscript received November 19, 1990; revised September 4, 1991. This work was supported by King Abdulaziz City for Science and Technology (KACST) Grant AR-5/29.

The authors are with the Electrical Engineering Department, College of Engineering, King Saud University, Riyadh 11421, Saudi Arabia.

IEEE Log Number 9200358.

Unfortunately, almost all the data reported in the published literature are taken in climatic regions that differ widely from the arid land climate of Saudi Arabia. In order to efficiently utilize the new frequency band, a propagation study in arid land is urgently needed. Such a study should be conducted over a span of several years, to obtain a sufficient statistical data. The study of millimetric wave propagation in Saudi Arabia is addressed in the present paper.

A glance over the rain data available for Riyadh city shows that, for most of the year, there is very little rainfall [4], and hence rain attenuation may not be the dominant propagation factor. On the other hand, sand and dust storms may occur several times each year. Particle sizes may range from a fraction of a micron to few hundred microns in radius. Due to the heavy particles of sand storms, which are never less than 0.04 mm in radius [5], the air—2 m above the earth's surface—could be clear of sand. Hence, we may expect that radio links will not be affected by sand storms. However, dust storms comprising much smaller particles (less than 0.01 mm in radius) may be found at as high as 100 m or more. This will reduce the visibility and affect the propagation in millimetric wave band [6]–[12]. A knowledge of the particle's shape, the size distribution, and the refractive index is needed to obtain the attenuation and cross polarization due to dust particles. Multipath fading due to temperature and pressure gradients is also expected to affect the propagation in Saudi Arabia.

II. Experimental System Description

A block diagram of the experimental system is shown in Fig. 1. The system comprises radio links, meteorological instrumentation and data acquisition, and processing system. Two millimeter wave links operating at 40 GHz and a near infrared link at 0.88 μm are shown. The millimeter wave transmitters and receivers are placed at 100 and 25 m above ground, respectively. Both the transmitter and receiver for the IR link are at 25 m above ground. The two millimeter-wave links share the same path for protection against equipment failure. Tone modulation is used for the millimeter-wave radios whereas a videos test signal, colour bar, is transmitted over the IR link.

The meteorological instruments are situated at the receiving site and include dust passive collectors (DPS) and high volume samplers (HVS) at different heights above ground. A particle-size-analyzer (PSA), used for measuring and analyzing dust particle size and distribution. Visibility reduction is measured using the near infrared link. A rainfall rate gauge

0018-926X/92$03.00

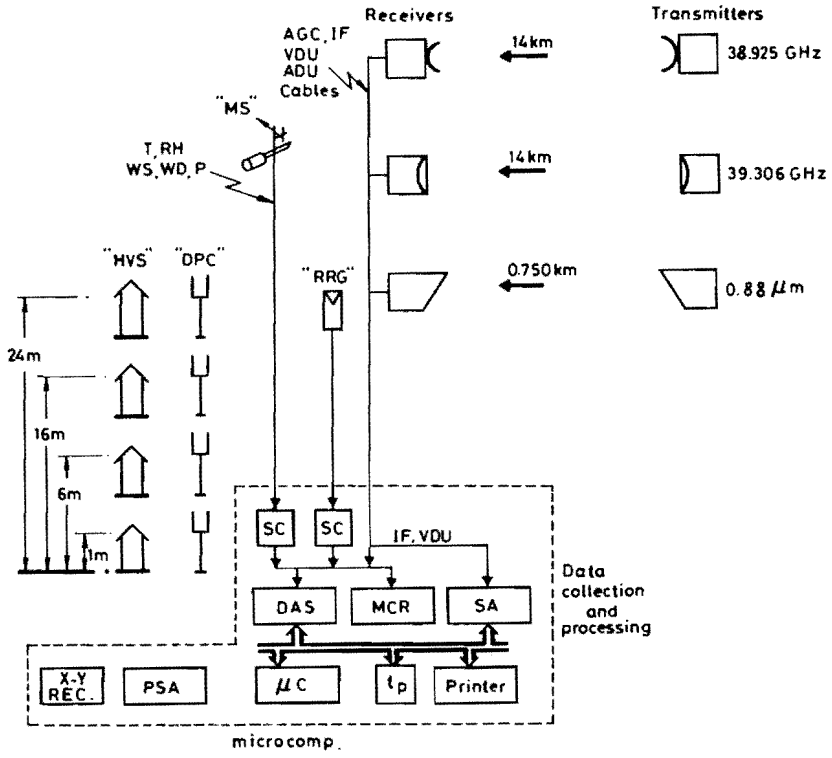

Legend
AGC : automatic gain control
DPC : dust-passive collector
VDU, ADU: video , audio
HVS : high volume sampler
RRG : rain rate gauge
DAS : data acquisition system
PSA : particle-size analyzer
SC : signal conditioner
MS : meteorological station
t_p : tape recorder

Fig. 1. Block diagram of the experimental system. AGC: automatic gain control; DPC: dust-passive collector; VDU, ADV: video, audio; HVS: high volume sampler; RRG: rain rate gauge; DAS: data acquisition system; PSA: particle-size analyzer; SC: signal conditioner; MS: meteorological station; t_p: tape recorder.

(RRG) with 1 min integration time and a meteorological station (MS) are shown as well. The meteorological station is equipped for measuring temperature (T), relative humidity (RH), wind speed and direction (WS, WD) and parameteric pressure (P). The data handling equipment include a microcomputer (μC), a tape recorder (t_p), a printer, a data acquisition system (DAS), a 40 GHz spectrum analyzer (SA) and a multichannel/recorder (MCR). The main parameters of the radio links are shown in Table I. The following is a brief description of the meteorological sensors used in the measurements.

- The high volume sampler is an active dust collector which consists of an air motor/blower of constant air flow, a glass fiber filter, and a manometer. Dust/sand particles are collected and deposited on the filter. By measuring the air flow and particle mass, dust concentration can be calculated.
- The particle size analyzer consists mainly of a sensitive (0.5 μg) electrobalance, sedimentation unit and a chart recorder. Particle-size distribution is calculated from the chart record of accumulated weight of settled particles and time using Stocke's law.

TABLE I
PARAMETERS OF RADIO LINK EQUIPMENT

Parameter	Radio Equipment		
	Hughes	NEC	IR
Transmitter frequency (GHz)	39.306/39.434	38.925	0.88 μm
Transmitted power (dBM)	+23	+10	+15
Transmitted type	DRO & Impatt	Impatt	GaAlAs
Polarization	Vertical	Vertical	Random
Antenna type	Cassegrain	Cassegrain	Fresnel lens
Antenna size (cm)	23	36	15.3 × 15.3
Antenna gain (dB)	35	40	—
Beamwidth (degree)	2.5	1.6	0.17 divergent
Receiver type	SH	SH	Silicon APD
Radome	Kapton (0.1 mm)	No	Glass
Bandwidth (MHz)	42.5 ± 2.5	35	40 nm

NEC = Nippon Electric Co., IR = Infrared, DRO = Dielectric resonator oscillator, APD = Avalanche photo diode, SH: Superhetrodyne.

- The rain rate gauge is a fast response gauge with one minute integration time and photoelectric drop counter, corresponding to a precipitation rate of 100 mm/h. It has a collecting area of 300 cm^2 and a sensitivity of 0.0083 mm of rain drop.

The dust passive collectors are open top cylinders of specified size and material. They have the advantage of simplicity and can collect the total settleable particles of sizes larger than the capability of active collectors.

The radio channels were scanned once each second whereas the mateorological sensors were scanned once each ten seconds. During the course of the experiment, more than 5000 h of reliable data were collected. However, only variations of more than 0.25 dB in signal level and more than 20% in meteorological parameters were retained for further processing.

III. Measured Visibility and Attenuation Due to Sandstorms

This section summarizes the measured sand/dust storm parameters and their effect on signal level of both the millimetric wave and infrared radio links. During the course of measurements, which spanned the period of 1985 to 1988, 10 sand/dust storms, on the average, were experienced in the city of Riyadh each year. Various meteorological parameters as well as received signal levels were recorded during storm events. For most of the events, the cell size of the storm exceeded 20 km. The mean temperature, relative humidity, vapor pressure, and wind speed were about 34°C, 59%, 1.4 KP_a, and 20 m/s, respectively. It was observed that a relatively high rate of change of the meteorological parameters occurred simultaneously with sand/dust storms.

A. Visibility Distribution

Fig. 2 shows the cumulative distribution of the optical visibility based on attenuation data measured for the infrared radio link during 1985–1988. The data represent a complete record of 41 blown dust and sand storm events experienced during the measurements period in the city of Riyadh. The figure also shows the average visibility distribution based on 20-year visibility data (1968–1987) obtained from the records of the Meteorological and Environmental Protection Administration (MEPA) in Riyadh. The record includes all events during which optical visibility was reduced below 10 km as a result of sand/dust storms in Riyadh. Visibility was measured by using the known marked distance method applied at several meteorological stations in Riyadh area. The measured visibility using the near infrared (NIR) radio link was obtained by utilizing the known relation between visibility and optical attenuation. Visibility may be defined as that distance from an observer at which a minimum contrast ratio C between a black object and a bright background is equal to $|C| = 0.02$. Such a value of $|C| = 0.031$ was proposed by Middleton [13] and yields a close agreement between the measured attenuation at infrared frequency and the optical visibility measured subjectively using the marked distance

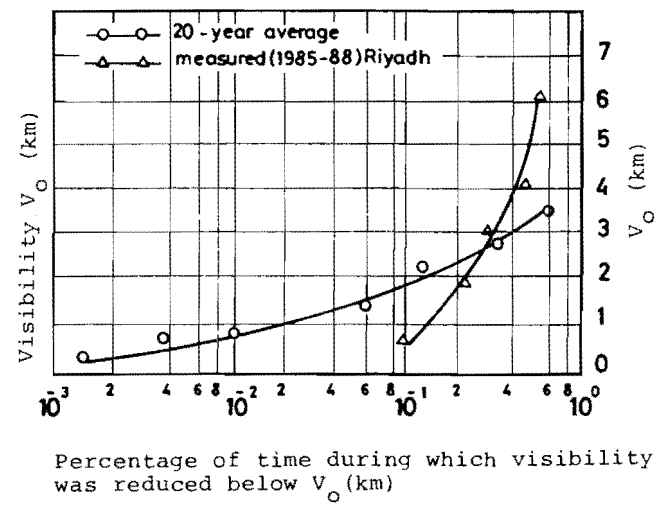

Fig. 2. Cumulative distribution or reduced visibility due to sandstorms in Riyadh.

method. The visible range, or visibility is related to the optical attenuation by the relation:

$$V_0 = \frac{4.343}{\alpha_0} \ln \left| \frac{1}{C} \right| \tag{1}$$

where V_0 is the visibility in kilometers and α_0 is the optical attenuation in decibel/kilometer. For $C = 0.31$, we get

$$V_0 = \frac{15}{\alpha_0}. \tag{2}$$

Although a power law, as well as an exponential relation, can closely approximate the probability distribution of the optical visibility, a log-normal fit yielded the best fit for the visibility data.

B. Attenuation due to Sand/Dust Storms

Table II presents the attenuation data due to sandstorms measured on both the 40 GHz (14 km) and the 0.88 μm (0.75 km) links in Riyadh.

Fig. 3 depicts the results of fitting the measured attenuation statistics on the 40 GHz as well as the 0.88 μm infrared radio links. Using a least-square error minimization algorithm for the fitting, the probability density function of the measured specific attenuation α(dB/km) is given by the exponential law:

$$P(\alpha) = 0.01 \exp(-14\alpha),$$

$$40 \text{ GHz}, \ \alpha < 0.5 \text{ dB/km} \tag{3a}$$

$$P(\alpha_0) = 0.01 \exp(-3\alpha_0/16),$$

$$0.88\mu\text{m}, \ \alpha_0 < 28 \text{ dB/km}. \tag{3b}$$

To obtain (3) from the data of Table II, two assumptions are made. First, the sandstorm occurs over the entire hop

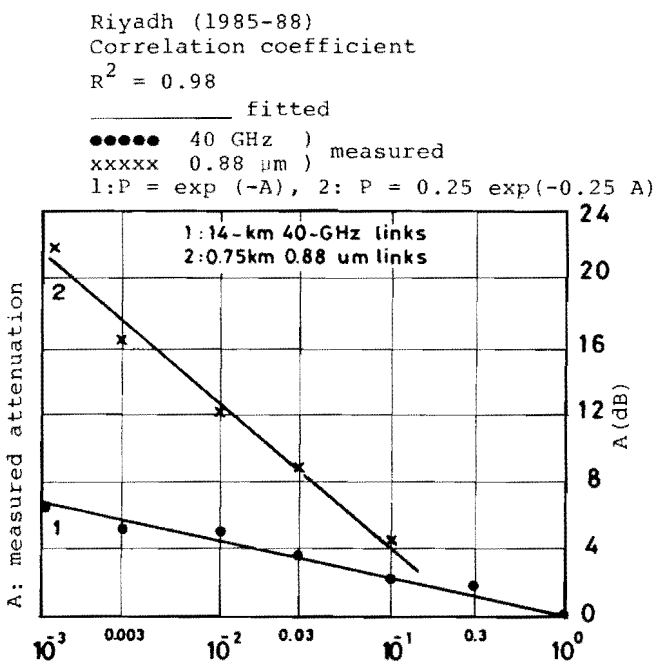

Fig. 3. Fitted attenuation distribution due to sandstorms for the 40 GHz and 0.88 μm radio links.

TABLE II
MEASURED ATTENUATION DUE TO SANDSTORMS IN RIYADH (1985-1988)

Percentage of time attenuation exceeded	1	0.3	0.1	.03	.01	.003	.001
A(dB)—40 GHz 14 km link	—	1.25	2.4	3.5	4.5	6	7
A(dB)—0.88 μm 0.75 km link	—	—	4	8.5	12	17	22

distance of 14 and 0.75 km for the 40 GHz and 0.88 μm links, respectively. The second is the occurrence factor of sandstorms, defined here as the probability of a sandstorm with visibility less than 10 km. The average value of the occurrence factor is about 0.01 during the course of the experiment.

C. Comparison of Measured and Calculated Attenuation

Based on the analysis of [1], [6], the attenuation of radio waves propagating through airborne sand particles of permittivity ϵ and effective radius a_e is given by

$$\alpha = 0.1887 \times 10^3 \left(\frac{a_e}{\lambda}\right) G \frac{1}{V_0} \quad \text{dB/km} \qquad (4)$$

where $G = 3\epsilon''/[(\epsilon' + 2)^2 + \epsilon''^2]$; $\epsilon = \epsilon' + j\epsilon''$ and a_e is the ratio of the third to second moments of the particle size distribution given by

$$a_e = I_3/I_2, \quad I_n = \int_0^\infty a^n f(a)\, da$$

TABLE III
COMPARISON OF MEASURED AND CALCULATED ATTENUATION DUE TO SANDSTORMS

Percentage of time attenuation exceeded	Measured attenuation		Calculated attenuation A_c for various moisture content		
	α(dB/km)	α_0(dB/km)	5%	10%	20%
0.1	0.164	13.0	0.041 (4)*	0.066 (2.5)	0.078 (2.1)
0.22	0.115	8.6	0.027 (4.2)	0.0435 (2.6)	0.051 (2.25)
0.3	0.0875	6.4	0.021 (4.3)	0.033 (2.65)	0.039 (2.1)
0.4	0.0684	4.9	0.153 (4.46)	0.024 (2.77)	0.0294 (2.32)

* The number (·) is the ratio A_m/A_c.

and $f(a)$ is the particle size distribution. V_0 is the visibility in kilometers and λ is the wavelength measured in the same units as the particle size a_e.

Table III compares the measured and theoretical attenuation due to sandstorms as calculated from (3) and (4). The particle size-distribution measured during sandstorms showed an exponential distribution with an average diameter of about 20 μm at a height of 15 m. For exponential distribution, the effective radius a_e is equal to $3a$, where a is the average radius. If we use the values of ϵ as in [14], the permittivity factor G can be calculated for various moisture content of the sand particles.

The measured and calculated attenuation due to airborne sand/dust particles shown in Table III for the 14 km hop at 40 GHz in Riyadh are of the same order of magnitude. However, the measured attenuation is two to four times larger than the calculated attenuations at a moisture contents of 20 and 5%, respectively. Even a large moisture content of 20% is unlikely to occur, particularly at a dry climate of relative humidity less than 60% as in Riyadh.

Since particle size and distribution are accurately measured and the permittivity factor of airborne dust is not greater than that of the mother soil [15], we have to turn our attention to a different mechanism that may cause such variation between measurements and calculations of attenuation.

In (3a) and (3b) and in Table II, uniformity of the sand particle distribution along the path was implied. For the 0.75 km link this is acceptable, however, for the 14 km link it may lead to an error. Analysis of the point measurements of particle-size distribution (at the receiving end) is taken as a representative over the 14 km link. However, the variability of particle-size concentration along the path at any instant of time is a possible cause of disagreement between analysis and measurement.

IV. MEASURED RAIN RATE AND RAIN ATTENUATION

This section presents the results of measuring rain rate and rain attenuation for the period 1986-1988 in the city of Riyadh, both at 40 GHz and at infrared wavelength (0.88 μm). Rain rate is measured at the receiver station and at a point along the path 10 km from the receiver. Since the hop length for the infrared link is only 0.75 km, it is assumed that

the entire hop is in rain during a rain event. Our aim is to find amplitude and duration statistics of rain rate and rain attenuation and to find the average rain cell size in the arid climate of Riyadh, Saudi Arabia. The results of measurements are compared with rain rate data obtained from several meteorological stations in Riyadh over a span of 25 years.

A. Rain Rate Amplitude Statistics

The rain seasons during the years 1986–1988 extended from January to April with a yearly average of 3190 min of rain rate in excess of 1 mm/h. Hence, the rain occurrence factor, based on the recording period, is about 6×10^{-3}. The rain rate statistics is given in Table IV, based on the average of two rain rate gauges operated simultaneously.

The percentage of time, during rain, in which the rain rate exceeds r mm/h can be well represented by a log-normal or an exponential relation. For an exponential fit we have:

$$Y(r) = \exp(-0.2r), \quad 1 < r < 40 \text{ mm/h} \tag{5}$$

and the measured probability of exceeding a rain rate of r mm/h is given by

$$P_m(r) = 6 \times 10^{-3} \exp(-0.2\ r), \quad 1 < r < 40 \text{ mm/h} \tag{6}$$

in which the 6×10^{-3} represents the rain occurrence probability. The above equations are obtained by fitting the data of Table IV using minimum-squared-error fitting algorithm. The correlation coefficient for the fitting is $R^2 = 0.99$.

Similar rain rate distributions were recorded by the two gauges for rain rates smaller than 25 mm/h. Wide differences, however, were observed for rates higher than 30 mm/h. Such a result may be explained by the cell size concept. Light rain tends to be wide spread with large cells, hence, both rain gauges may receive nearly equal rain for low rain rates such that $r < 35$ mm/h. On the other hand, intense rain tends to be more localized, with a decreasing cell size, as intensity is increased.

B. Rain Rate Duration Distributions

The number of minutes $T(r)$, during rain, for which the average rain rate is r min/h is also analyzed. It is found that both exponential and normal laws can closely represent the event duration data. For the normal fitting we have:

$$T(r) = 420 \exp\left[-0.4(r - 45)^2\right] \text{ min}, \quad 0 < r < 40 \text{ mm/h}. \tag{7}$$

The above results are useful in describing the nature of rain in arid climate. However, the rain occurrence factor varies widely from year to year, since rain pattern is rather irregular in arid land, marked by low rainfall.

C. Long-Term Rain Fall Data

Rainfall intensity data for the period 1963–1987 consists of records from 137 recording rainfall stations in Saudi Arabia.

TABLE IV
MEASURED RAIN RATE STATISTICS FOR RIYADH (1985–1988) AND 25 YEAR AVERAGE (1963–1987)

Percentage of rain time for which rain rate exceeded	1	0.3	0.1	0.03	0.01	0.003	0.001
Measured rain rate r(mm/h) (1985–988)	1	6	12	17	24	30	36
The 25-year average rain rate (mm/h) (1963–1987)	3.5	10	25	38	50	60	75

These data represent the intensity portion of the rainfall data collected by the Hydrology Division, Ministry of Agriculture and Water (MAW).

The amount of rainfall that falls over Riyadh is very irregular through the years and through the months. The minimum rainfall occurred in 1970 with an amount of 12.6 mm, while the maximum occurred in 1976 with an amount of 176.6 mm. Average annual rainfall is 81.2 mm.

Rainfall occurs mainly in winter and spring months. Summers are dry, with practically no rainfall, while autumn months receive very little rain. About 95% of the rainfall occurs during the winter and spring months. For arid types of climates, the average rainfall is less than 200 mm/year.

Rain attenuation is related to rain rate in millimeters/hour rather than rainfall intensity in millimeters, hence it is necessary to transfer the available rainfall data into rain rate as described in [16]. Once rainrate data has been obtained, several probability laws were considered to represent the data. Table IV shows the rain rate statistics based on 25-year (1963–1987) rain rate data for Riyadh. Best fit was obtained using log-normal and exponential distributions. The yearly probability of exceeding a rain rate of r mm/h is found as

$$P(r) = 1.1 \times 10^{-3} \exp(-0.1r), \quad 1 < r < 75 \tag{8}$$

in which the 1.1×10^{-3} represents the rain occurrence factor, averaged over 25 years in Riyadh. Fig. 4 depicts the 25-year average distribution of (8), together with the measured distribution of (6). 4–5

D. Measured Attenuation Due to Rain

Excess attenuation due to rain was recorded during the measurement period 1986–1988. Two millimetric wave radio links operating at 40 GHz over a hop of 14 km length were monitored for attenuation together with a 0.75 km, hop link operating at the near infrared wavelength of 0.88 μm. Statistical analysis of fade amplitude and duration are prepared. Our goal is twofold. First we are interested in such fade statistics to study the effect of rain storms on link availability in arid land. Second, a comparison of attenuation and rain rate statistics may be used to determine the value of the a, b parameters in the frequently used relation between rain rate R and rain attenuation A where

$$A(\text{dB/km}) = aR^b(\text{mm/h}). \tag{9}$$

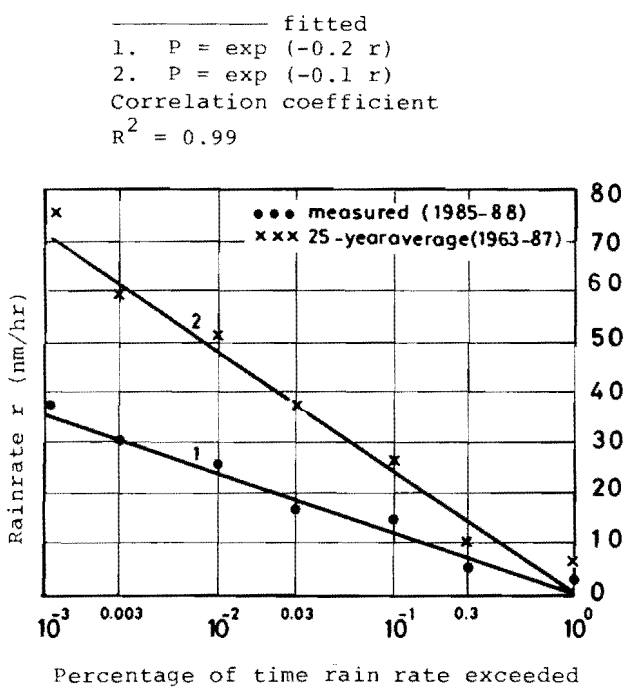

Fig. 4. Rain rate distribution for Riyadh.

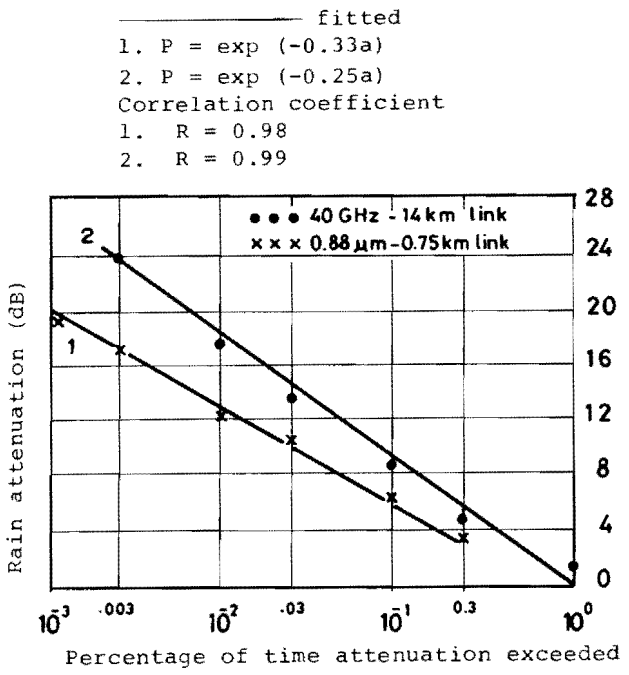

Fig. 5. Distribution of measured rain attenuation in Riyadh.

Since attenuation statistics are obtained for hop lengths of 14 km and 0.75 km, cell size at various rain rates can be estimated. Table V presents rain attenuation statistics for both the millimetric wave and infrared radio links.

The above rain attenuation data can be well represented by exponential or log-normal laws. The probability of exceeding a fade depth of a dB is given by

$$P(a) = 6 \times 10^{-3} \exp(-0.25a), \quad 14 \text{ km} - 40 \text{ GHz}, 1 < a < 28 \text{ dB} \quad (10a)$$

TABLE V
MEASURED RAIN ATTENUATION STATISTICS FOR 40 GHz AND 0.88 μM LINKS IN RIYADH (1985-1988)

Percentage of time during rain for which attenuation exceeds a (dB)	1	0.3	0.1	0.03	0.01	0.003	0.001
a(dB): measured on on 14 km—40 GHz link	1	5	9	14	18	24	> 24
a_0(dB): measured on 0.75 km—0.88 μm link	3.5	10	25	38	50	60	75

$$P(a_0) = 0.25 \times 6 \times 10^{-3} \exp(-0.33a_0), \quad 0.75 \text{ km} - 0.88 \ \mu\text{m}, 3.5 < a_0 < 20 \text{ dB} \quad (10b)$$

The factor 6×10^{-3} in (10) is the probability of rain (rain occurrence factor). The additional 0.25 factor in (10b) shows that only 0.25 of the rain period caused appreciable attenuation on the infrared link. This observation will be further investigated in the following section.

E. Comparing Measured and Calculated Attenuation

Comparison of the measured and calculated attenuation due to rain at infrared wavelength reveals the following.

First we observe that the probability of occurrence of rain attenuation at 0.88 μm wavelength is smaller by a factor of 0.25 than that of rain rate in excess of 1 mm/h as given by (5). The 0.25 probability corresponds to a rate of > 7 mm/h, hence, it seems that rain events with rates < 7 mm/h did not cause appreciable attenuation on the infrared link. To further investigate this interesting observation, the relation between rain rate, and excess attenuation is given by [17].

$$a_c(\text{dB/km}) = 0.912 R^{0.74}(\text{mm/h}), \quad \text{at } 0.88 \ \mu\text{m} \quad (11)$$

from which a rain rate of 7 mm/h is expected to cause an attenuation of 2.88 dB over a 0.75 km hop at 0.88 μm wavelength. Since all attenuations in excess of 2 dB were recorded by the system, it seems that an explanation is needed as to why a rain rate of < 7 mm/h went unnoticed by the infrared radio link? We may answer the question by recalling that typical raindrops of a size > 100 μm are quite large compared to infrared wavelength, hence, the size parameter $(a/\lambda) \gg 100$. As a result, the scattering from such large objects tends to be highly concentrated in the forward direction, and therefore, increases signal power at the receiver. The measured attenuation α_m is, thus, smaller than the calculated α_c as given by the relation:

$$\alpha_m = \alpha_c(1 - \rho) \quad (12)$$

where ρ is the forward scattering correction factor. An increase in raindrop size from 250 to 3000 μm causes ρ to increase from 0.1 to 0.3 [18]. Since light rain and drizzle are marked by smaller drops than heavy showers [19], [20], ρ is larger for lower rain rate and α_m is proportionally smaller.

Now, choosing $\rho = 0.3$ reduces the calculated attenuation from 2.88 to about 2 dB, which was not recorded by the

system. From the above discussion it seems that the relation $A = aR^b$ as given in (11) for 0.88 μm predicts attenuation fairly accurately at optical wavelength (there is no appreciable change of attenuation by rain at the optical wavelength). An interesting observation is that attenuation caused by light rain is further deemphasized at optical wavelength due to forward scattering correction factor.

The above results have direct application in millimeter-wave radio design, especially in arid climate. For areas of the globe with heavy rainfall, short hops must be used at extremely high frequency in order to meet the required reliability objectives. For dry regions, however, longer hops can be used to reduce total cost and probability of outage due to equipment failure. Unlike the short hop case, where the rain cell may cover the entire hop, knowledge of the rain cell-size is essential for air climate with a possibility of extended hop length at higher radio frequencies. Remote sensing of earth parameters at frequencies higher than 10 GHz, where rain attenuation affects the validity of measurements, is another area of concern. Here, the cell-size information may be used for correcting the obtained data [21].

V. Conclusion

A field study aimed at studying the propagation of millimeteric waves in aridland was under way in the city of Riyadh for a period of four years. The paper presented the results of measuring signal attenuation caused by sand/dust storms and rain at 40 GHz and near infrared frequencies. Various meteorological parameters were simultaneously measured and statistically analyzed with emphasis on visibility and rain rate. The essence of the results can be summarized as follows.

1) Attenuation caused by sand/dust storms occurred for 1%. of the experiment time and with an exponentially decreasing probability that a given fade depth is exceeded (3).

2) The assumption of a uniform particle size distribution along the path tends to underestimate the excess attenuation due to sandstorms by a factor of 2 to 4. Particle size distribution should be measured at several points along the path in order to correctly predict excess attenuation using visibility measurements and the single-scattering model. Scintillation fading caused by variations in the meteorological parameters coupled with large variations in the refractive index of the atmosphere during sand storms can increase the signal attenuation as well. This may also explain the larger attenuation experienced during sand/dust storms as shown in Table III.

3) Rain events occurred for about 0.6% of the total measuring time and during rain events the probability that rain rate exceeds r mm/h decreases exponentially with 0.2 r. On the other hand, the rain rate duration resembles a normal distribution as given in (7).

4) Based on 25-year rain data for several recording stations in the Riyadh area rain events occurred for about 0.11% of the time with exponentially decreasing probability of exceeding r mm/h as given in (8).

5) The statistics of measured attenuation due to rain are given by (10) for both the 40 GHz and the near-infrared radio links. At infrared, the measured rain attenuation was found smaller than the calculated, however, using a forward scattering correction factor ρ (12) of 0.3 yields close agreement between the measured and calculated attenuation.

Although reliability and outage analysis are not included in this paper, such an analysis can be easily pursued based on the complete statistics of rain attenuation and sand storms. It can also be verified that the two factors viz., sand storm and rain play equally important roles in determining the link reliability for long hops in arid climate.

Acknowledgment

The authors are indebted to the reviewer who brought to our attentions the role of nonuniformity of particle-size distribution along the path as explained at the end of section III.

References

[1] J. Goldhirsh and R. L. Robinson, "Attenuation and space diversity statistics calculated from radar reflectivity data of rain," *IEEE Trans. Antennas Propagat.*, vol. AP-30, Nov. 1982.

[2] Y. Mori, I. Higuti, and K. Morita, "Estimation of effect of frequency band diversity on earth-satellite links in microwave and millimeter wave bands," *Electron. and Commun. in Japan*, vol. 61-B, no. 10, pp. 55-61, 1978.

[3] J. Neves and P. A. Watson, "Cross-polarization, differential attenuation and differential phase shift measured on a 36.5 GHz terrestrial link," URSI Commission F Symp., Canada, preprints, pp. 5.1.1-5.1.6, 1980.

[4] Ministry of Agriculture and Water, "Water resources and development," Hydrology Div., Pub. 96, p. 40, 1980.

[5] R. A. Bagnold, *The Physics of Blown Sand and Desert-Dunes*. Chapman & Hall, 1973.

[6] A. J. Ansari and B. G. Evans, "Microwave propagation in sand and dust storms," *Inst. Elec. Eng. Proc., VI*, vol. 129, pt. F, no. 5, 1982.

[7] T. S. Chu, "Effect of sand storms on microwave propagation," *Bell Syst. Tech. J.*, vol. 58, pp. 549-555, 1979.

[8] H. T. Al-Hafid, S. C. Gupta, M. Al-Mashadani, and K. Buni, "Study of microwave propagation under adverse dust storm conditions," presented at Third World Telecommun. Forum, Geneva, 1979.

[9] C. J. Gibbins and M. G. Pike, "Millimetre, infrared and optical propagation, studies on a 500 m range," 5th Intl. Conf. Antennas Propagat., pt. 2, ICAP-87, York, U.K., 1987, pp. 50-53.

[10] J. Goldhirsh, "A Parameter review and assessment of attenuation and backscatter properties associated with duststorms over desert regions in the frequency range of 2 to 10 GHz," *IEEE Trans. Antennas Propagat.*, vol. AP-30, pp. 1122-1127, Nov. 1982.

[11] S. I. Ghobrial and S. M. Sharief, "Microwave attenuation and cross polarization in duststorms," *IEEE Trans. Antennas Propagat.*, vol. AP-35, pp. 418-425, 1987.

[12] S. O. Bashir and N. J. McEwan, "Crosspolarization and gain reduction due to sand or dust on microwave reflector antennas," *Electron. Lett.*, vol. 21, no. 9, pp. 379-380, Apr. 25, 1985.

[13] W. E. K. Middleton, *Vision through the Atmosphere*. Toronto, Canada: Univ. Toronto Press, 1952.

[14] CCIR Recommendation 453, Rep. 563-1, 1990.

[15] F. Geiger and D. Williams, "Dielectric Constants of Soils at Microwave Frequencies," NASA/Goddard Space Flight Center, Greenbelt, MD, Rep. X-652-72-238, 1972.

[16] A. A. Ali, "Millimeter wave propagation in Arid Land—The effect of rain and sandstorms," *Int. J. Infrared and Millimeter Waves*, vol. 7, no. 3, pp. 323-337, 1986.

[17] V. E. Zeuv, *Laser Beams in the Atmosphere*. New York: Consultant Bureau, 1982.

[18] T. S. Chu and D. C. Hogy, "Effects of precipitation on propagation at 0.63, 3.5 and 10.6 microns," *Bell Syst. Tech. J.*, vol. 47, no. 5, pp. 723-759, 1980.

[19] E. J. McCartney, *Optics of the Atmosphere*. New York: Wiley, 1976.

[20] M. P. M. Hall, *Effects of Troposphere on Radio Communication*. London, U.K.: Peregrinus, 1979, pp. 42-43, p. 103.

[21] J. Goldhirsh, "Rain cell size statistics as a function of rain rate for attenuation modeling," *IEEE Trans. Antennas Propagat.*, vol. AP-31, pp. 779-801, Sept. 1983.

Adel A. Ali received the B.Sc. degree from Alexandria University, Egypt, in 1967 and the M.Sc. and Ph.D. degrees from the University of Manitoba, Canada, in 1973 and 1976, respectively, all in Electrical Engineering.

From 1976 to 1978, he was a Transmission and Special Services Engineer with Manitoba Telephone Systems, Winnipeg, Canada. Since 1978, he has been with the Electrical Engineering Department, King Saud University, Riyadh, Saudi Arabia where he is now a Professor. His research interests include communication theory, secure communication, mobile radio and microwave propagation.

Mohammed A. Alhaider (S'71-M'82-SM'84) received the B.Sc. degree from King Saud University, Riyadh, Saudi Arabia, in 1968, and the M.Sc. and Ph.D. degrees from Carnegie-Mellon University, Pittsburgh, PA, in 1972 and 1977, respectively, all in electrical engineering.

Since 1977 he has been with the College of Engineering, King Saud University, where he is currently a Professor of Electrical Engineering at the College of Engineering, King Saud University. He was Deputy Dean from 1979-1982, Dean from 1982-1985, and the supervisor of DPC from 1985 to 1987. His areas of interest include engineering education in developing countries, optical and microwave communications, and acoustooptic interactions in thin films.